Aquat Geochem (2016) 22:225–251
DOI 10.1007/s10498-016-9290-6

ORIGINAL ARTICLE

Understanding the Cyclicity of Chemical Weathering and Associated CO_2 Consumption in the Brahmaputra River Basin (India): The Role of Major Rivers in Climate Change Mitigation Perspective

Pallavi Das[1] · Kali Prasad Sarma[1] · Pawan Kumar Jha[2] · Rajnish Ranjan[3] · Roger Herbert[4] · Manish Kumar[1]

Received: 27 August 2015 / Accepted: 31 March 2016 / Published online: 20 April 2016

Abstract Weathering of rocks that regulate the water chemistry of the river has been used to evaluate the CO_2 consumption rate which exerts a strong influence on the global climate. The foremost objective of the present research is to estimate the chemical weathering rate (CWR) of the continental water in the entire stretch of Brahmaputra River from upstream to downstream and their associated CO_2 consumption rate. To establish the link between the rapid chemical weathering and thereby enhance CO_2 drawdown from the atmosphere, the major ion composition of the Brahmaputra River that drains the Himalaya has been obtained. Major ion chemistry of the Brahmaputra River was resolved on samples collected from nine locations in pre-monsoon, monsoon and post-monsoon seasons for two cycles: cycle I (2011–2012) and cycle II (2013–2014). The physico-chemical parameters of water samples were analysed by employing standard methods. The Brahmaputra River was characterized by alkalinity, high concentration of Ca^{2+} and HCO_3^- along with significant temporal variation in major ion composition. In general, it was found that water chemistry of the river was mainly controlled by rock weathering with minor contributions from atmospheric and anthropogenic sources. The effective CO_2 pressure ($\log P_{CO_2}$) for pre-monsoon, monsoon and post-monsoon has been estimated. The question of rates of chemical weathering (carbonate and silicate) was addressed by using TDS and run-off (mm $year^{-1}$). It has been found that the extent of CWR is directly dependent on the CO_2 consumption rate which may be further evaluated from the perspective of climate change

Electronic supplementary material The online version of this article (doi:10.1007/s10498-016-9290-6) contains supplementary material, which is available to authorized users.

✉ Manish Kumar
manish.env@gmail.com

[1] Department of Environmental Science, Tezpur University, Napaam, Assam 784028, India

[2] Centre of Environmental Studies, University of Allahabad, Allahabad, Uttar Pradesh 211002, India

[3] Kameng Hydroelectric Project, North Eastern Electric Power Corporation (NEEPCO), West Kameng, Arunachal Pradesh, India

[4] Department of Earth Sciences, Uppsala University, Villavägen 16, 752 36 Uppsala, Sweden

mitigation The average annual CO_2 consumption rate of the Brahmaputra River due to silicate and carbonate weathering was found to be 0.52 ($\times 10^6$ mol Km^{-2} $year^{-1}$) and 0.55 ($\times 10^6$ mol Km^{-2} $year^{-1}$) for cycle I and 0.49 ($\times 10^6$ mol Km^{-2} $year^{-1}$) and 0.52 ($\times 10^6$ mol Km^{-2} $year^{-1}$) for cycle II, respectively, which were significantly higher than that of other Himalayan rivers. Estimation of CWR of the Brahmaputra River indicates that carbonate weathering largely dominates the water chemistry of the Brahmaputra River.

Keywords Brahmaputra River · Water chemistry · Weathering · CO_2 consumption rate · Climate change

1 Introduction

Rivers are major components of the global water cycle which play an important role in the geochemical cycling of elements. Both natural and anthropogenic sources supply dissolved and particulate loads to rivers which are responsible for changing water chemistry. Chemical weathering is a dominant natural process that consumes atmospheric CO_2 and transforms it to dissolved HCO_3^- in continental waters. Thus, weathering of silicates and carbonates represent an important carbon sinks of varied scales (Li et al. 2011; Sun et al. 2010; Jha et al. 2009). The chemical composition of river water is of great importance for quantifying the dissolved load, pinpointing sources of major ions, estimating chemical weathering rates and associated CO_2 consumption (Das et al. 2005; Jha et al. 2009; Sharma and Subramanian 2008).

Studies on weathering and CO_2 consumption rate have been carried out worldwide, on watersheds, catchment areas and river basins. In India, studies on chemical weathering and CO_2 consumption rate chiefly focus on the large basins formed by the Himalayan (Sarin et al. 1989; Galy and France-Lanord 1999; Singh et al. 2006) and Peninsular rivers (Dessert et al. 2001; Das et al. 2005; Jha et al. 2009). The Himalayan rivers have been extensively used to study CO_2 consumption rate due to effect of tectonics and high physical erosion rate (Sarin et al. 1989; Krishnaswami et al. 2005). A large number of studies demonstrated that natural factors such as lithology, temperature, run-off, relief and vegetation are dominant controls of water chemistry (Gaillardet et al. 1999; Horowitz et al. 1999; Grasby and Hutcheon 2000; Millot et al. 2002). Since the Cenozoic period, origin and evolution of the Himalaya have contributed towards enhanced silicate weathering, thereby increasing CO_2 drawn from the atmosphere (Raymo et al. 1988). This accelerated chemical denudation rate due to high relief, high rainfall, melting of snow, rapid tectonic uplift and high stream power generate high rates of chemical change (Hren et al. 2007). Thus, the Himalayan rivers have received special but scattered attention in recent years for determining CO_2 consumption rate.

The Brahmaputra River, true to its Himalayan origins, experiences enhanced weathering due to rapid rock uplift, intense physical weathering and heavy monsoonal precipitation that enable it to consume an increased amount of CO_2 from the atmosphere (Singh et al. 2004, 2006). It was reported that this river transports 73 million tons of dissolved material annually, which accounts for approximately 4 % of the total dissolved flux to the world's ocean (Krishnaswami et al. 2005; Hren et al. 2007). Due to high chemical budgets of the Brahmaputra River, it is important to investigate its weathering and associated CO_2 consumption rate in order to estimate its influence on global CO_2 budget. In previous studies

involving estimation of CO_2 consumption and weathering rate, only one or two sample sites in Assam had been covered, and therefore, this is the first attempt to study the continuous stretch of the Brahmaputra River (from upstream (Guijan) to downstream (Dhubri)) covering both banks, aimed to arrive at a comprehensive understanding of weathering and CO_2 consumption rate of river and its contribution towards climate change mitigation.

The present study has been carried out with an objective to estimate the weathering and associated CO_2 consumption rate on the 891 km stretch of (from Guijan to Dhubri) Brahmaputra River during the two monsoon cycles with a gap of 1-year period from February 2011 to May 2014. The study also focuses on spatial and temporal variations, effect of monsoon, long-term comparison and shift in change of CO_2 consumption.

2 Study Area

The Brahmaputra River is the fifth largest river in the world (Berner and Berner 1996) with respect to discharge and second in terms of sediment transport per unit area (Milliman and Meade 1983). The River has high seasonal variation, a high sediment load, is characterized by frequent changes in channel position (Thorne et al. 1993). The Brahmaputra River originates on the Angsi Glacier, located on the northern side of the Himalayas in Burang County of Tibet, at an elevation of 5300 m above mean sea level (Sarin et al. 1989).

The Brahmaputra River has a drainage area of 580,000 km^2 (50.5 % in China, 33.6 % in India, 8.1 % in Bangladesh and 7.8 % in Bhutan) and an annual mean discharge of 510 km^3 (Subramanian 2004). The width of the river varies from 3 km to 18 km with an average of 10 km in the plains of Assam and Bangladesh. The Brahmaputra River is subjected to the Southeast Asian Monsoonal regime with a mean annual rainfall of 2300 mm out of which approximately 90 % of the rainfall occurs during the period from April to September. Because of abundant precipitation, erosion is at a maximum during this period. The geology of the Brahmaputra valley of Assam consists of the Higher and Lesser Himalaya sequences that consists of schists, marbles with amphibolites, and

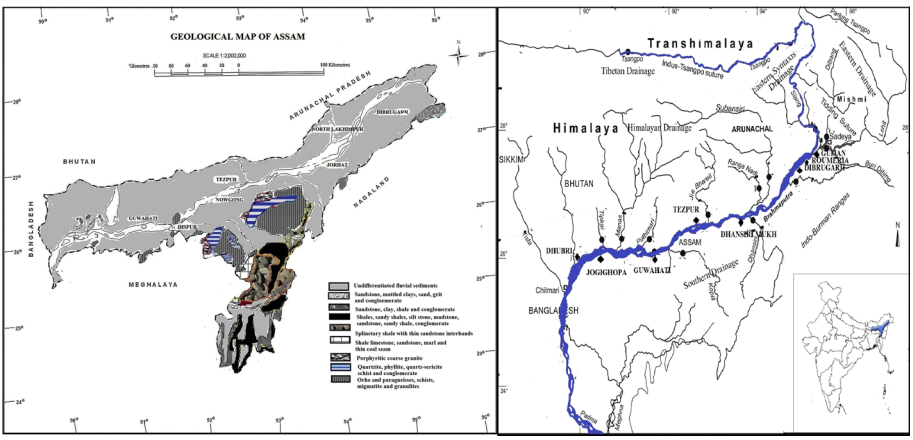

Fig. 1 Map of the study area illustrating the Brahmaputra River with sampling locations from Guijan to Dhubri (upstream to downstream)

quartzites (Sarin et al. 1989). The Brahmaputra system of Assam Plains consists of older and newer alluvium deposits. Alluvium formed during the Pleistocene age (older alluvium) is found in slightly undulating areas on both sides of the Brahmaputra River, the new alluvium soils near the river consist of alluvial materials washed down from the highland areas.

3 Materials and Methods

3.1 Sample Collection and Analytical Method

The river water samples ($n = 54$) were collected in three different seasons during 2011 to 2014—cycle I: pre-monsoon (February 2011), monsoon (September 2011) and post-monsoon (January 2012) followed by cycle II: pre-monsoon (April 2013), monsoon (December 2013) and post-monsoon (May 2014). The collection areas covered nine sites starting from upstream to downstream of the Brahmaputra River, i.e. Guijan, Romeria, Dibrugarh, Jorhat, Dhansiri Mukh, Tezpur, Guwahati, Jogighopa and Dhubri, as shown in Fig. 1. Water samples were collected in 250 and 125 ml polypropylene bottles. In 125-ml polypropylene bottle, water samples were filtered using 0.45-μm Millipore filters and preserved by acidification with HNO_3^- acid. In situ measurements included pH, electrical conductivity (EC) and total dissolved solid (TDS) which were measured using Multiparameter Water Quality Portable Meter (Hanna model-HI 9828) and bicarbonate (HCO_3^-) was measured by potentiometric titration method in unfiltered samples. For other parameters, samples were preserved in sampling kits maintained at 4 °C until analysis (Kumar et al. 2009b). The major ion analyses were conducted as per the standard methods prescribed by American Public Health Association 2005 [calcium (Ca^{2+}) and magnesium (Mg^{2+}) ICP-OES]; [sodium (Na^+) and potassium (K^+), flame photometer]; [phosphate (PO_4^{3-})], [dissolved silica (H_4SiO_4), sulphate (SO_4^{2-}), nitrate (NO_3^-),UV spectrophotometer]; [chloride (Cl^-), titration method]. Statistical analyses (ANOVA and PCA) were performed using SPSS version 22.0.

4 Results and Discussion

4.1 Spatio-Temporal Variation of Major Ions of the Brahmaputra River

4.1.1 Spatial Variation

There was not much variation in pH of river water and found to be slightly neutral to alkaline in nature. EC and concentration of TDS was found to be high in downstream location (B7 and B9) during pre-monsoon and post-monsoon seasons which may be due to various anthropogenic activities such as dredging, sand recovery, transportation of ferry, fishing, cremation on the banks and cultivation. High HCO_3^- concentration was found at S1 and S7 which may be due to seasonal and anthropogenic factors. SO_4^{2-} concentration was maximum at B5 and B8; its increase towards downstream of the river indicating anthropogenic influence. Cl^- concentration was found to be high at B5 and B6. Maximum NO_3^- and PO_4^{3-} content found in upstream locations could be attributed to the presence of several tea gardens and populated villages with cultivable land along the river bank.

Table 1 Statistical summary of the chemical composition of the Brahmaputra River water samples in pre-monsoon, monsoon and post-monsoon seasons for cycle I (2011–2012) and cycle II (2013–2014)

Variable	Pre-monsoon		Monsoon		Post-monsoon	
	Range 2011–2012	Range 2013–2014	Range 2011–2012	Range 2013–2014	Range 2011–2012	Range 2013–2014
(*a*)						
pH	6.45–7.95	7.03–8.46	7.0–7.72	6.48–7.92	7.38–8.24	7.23–7.87
EC (μS/cm)	167–272	129–147	81–162	105–198	92.6–160	102–192
TDS (mgL^{-1})	112–182	86.4–117	54.3–108	70.3–133	62.0–107	68.3–129
HCO_3^- (μM)	1721–2951	1081–2213	1230–1721	820–1967	984–1557	1147–1967
Cl^- (μM)	66.5–240	70.4–175	98.6–320	98.6–239	99.2–290	90.1–211
NO_3^- (μM)	18.4–19.7	18.1–19.8	19.0–19.8	17.7–27.4	18.1–20.0	18.1–29.2
SO_4^{2-} (μM)	108–216	39.6–229	131–437	107–396	36.7–107	97.9–216
PO_4^{3-} (μM)	0.46–0.87	0.64–2.31	0.41–1.03	0.31–1.54	0.44–0.67	0.54–1.54
H_4SiO_4 (μM)	13.6–41.4	30.3–120	33.3–127	42.2–148	1.27–45.8	25–70
Na^+ (μM)	235–426	239–450	226–539	274–504	187–491	283–478
K^+ (μM)	43.6–64.1	30.8–103	46.1– 64.1	53.8–97.4	38.5–59.0	56.4–100
Ca^{2+} (μM)	487–825	325–700	368–598	397–700	275–556	425–850
Mg^{2+} (μM)	200–475	175–442	137–340	137–283	107–257	117–258
TZ^+ (μEq)	1776–2946	1484–2363	1660–2092	1560–2233	1347–1969	1563–2535
TZ^+– (μEq)	2156–3494	1793–2498	1919–2532	1820–2644	1479–2048	1552–2469
Variable	Pre-monsoon		Monsoon		Post-monsoon	
	Avg ± SD 2011–2012	Avg ± SD 2013–2014	Avg ± SD 2011–2012	Avg ± SD 2013–2014	Avg ± SD 2011–2012	Avg ± SD 2013–2014
(*b*)						
pH	7.48 ± 0.41	7.36 ± 0.47	7.41 ± 0.22	7.58 ± 0.43	7.85 ± 0.30	7.91 ± 0.21
EC (μS/cm)	195 ± 31.2	147 ± 17.2	115 ± 26.0	139 ± 26.6	121 ± 21.9	135 ± 31.2
TDS (mgL^{-1})	138 ± 20.9	98.8 ± 11.6	91.4 ± 41.8	93.4 ± 17.8	58.3 ± 44.3	90.5 ± 20.9
HCO_3^- (μM)	2058 ± 385	1657 ± 321	1403 ± 156	1559 ± 334	1281 ± 180	1504 ± 258
Cl^- (μM)	145 ± 49.2	119 ± 35.6	180 ± 70.9	162 ± 43.3	178 ± 67.4	134 ± 36.8
NO_3^- (μM)	19.0 ± 0.54	18.8 ± 0.53	19.5 ± 0.24	21.3 ± 3.40	19.2 ± 0.66	20.5 ± 3.38
SO_4^{2-} (μM)	166 ± 36.1	229 ± 56.0	271 ± 111	396 ± 121	65.9 ± 24.9	216 ± 41.0
PO_4^{3-} (μM)	0.64 ± 0.14	1.22 ± 0.57	0.64 ± 0.20	0.80 ± 0.43	0.57 ± 0.07	1.0 ± 0.33
H_4SiO_4 (μM)	28.4 ± 9.34	62.6 ± 24.8	64.5 ± 29.0	82.7 ± 32.9	13.6 ± 14.0	42.2 ± 15.8
Na^+ (μM)	308 ± 61.7	329 ± 80.0	359 ± 104	338 ± 78.0	354 ± 95.4	360 ± 64.1
K^+ (μM)	51.8 ± 6.38	67.2 ± 21.5	55.8 ± 6.88	76.6 ± 15.6	47.5 ± 6.30	69.8 ± 12.3
Ca^{2+} (μM)	597 ± 102	494 ± 131	470 ± 73.1	533 ± 113	419 ± 86.1	636 ± 147
Mg^{2+} (μM)	277 ± 82.4	247 ± 79.3	254 ± 63.9	212 ± 47.8	186 ± 46.5	166 ± 43.0
TZ^+ (μEq)	2108 ± 349	1882 ± 270	1361 ± 209	1864 ± 141	1612 ± 206	2032 ± 346
TZ^+– (μEq)	2534 ± 416	2174 ± 233	2434 ± 143	2209 ± 216	1779 ± 182	1959 ± 257

SD standard deviation

Avg average

H_4SiO_4 content was found to be high at B9. Na^+ concentration was found to be high at B2 and B6, K^+ concentration was found to be higher at B1 and B8. The concentration of Ca and Mg shows increasing trend from upstream to downstream.

4.1.2 Temporal Variation

A comparative statistical summary of the Brahmaputra River water chemistry from different seasons during 2011–2012 (cycle I) and 2013–2014 (cycle II) is presented in Table 1. High pH value in pre-monsoon and post-monsoon seasons indicates the alkaline nature of the river. Fluctuations in pH values during different season of the year were attributed to factors such as removal of CO_2 by photosynthesis through bicarbonate degradation, dilution of water with freshwater influx, reduction in temperature and decomposition of organic matter (Rajasegar 2003). Average EC value was found to be high in pre-monsoon season and low in monsoon season. Maximum EC values for pre and post-monsoon seasons were due to high concentrations of dissolved salts and the presence of more alluvial-derived soil (entisol, inceptisol, alfisol) and less resistant minerals in the catchment area. Low EC values during monsoon may be due to dilution effect by rain water. TDS is derived from the chemical weathering of the basin. Average TDS values were found to be high during pre-monsoon season for both the cycles. It was found that in the post-monsoon season TDS values increased due to increase in dissolved minerals. A good correlation was found between EC and TDS indicating that EC is a measure of TDS.

Bicarbonate (HCO_3^-) was the dominant dissolved anion with an average value high in pre-monsoon and monsoon seasons for cycle I and cycle II, respectively, which are shown in Fig. 2. High level of alkalinity reflects bicarbonate is produced through mineral weathering and the influence of anthropogenic activity in the river system. Conversely, decreased HCO_3^- concentration was caused by low pH in post-monsoon season. Average Cl^- content was high in monsoon season for cycle I and cycle II which may be due to mixing of run-off water which carries larger quantity of salts from catchment area. Other possible sources of Cl^- are discharge of domestic and industrial waste to the river. It was

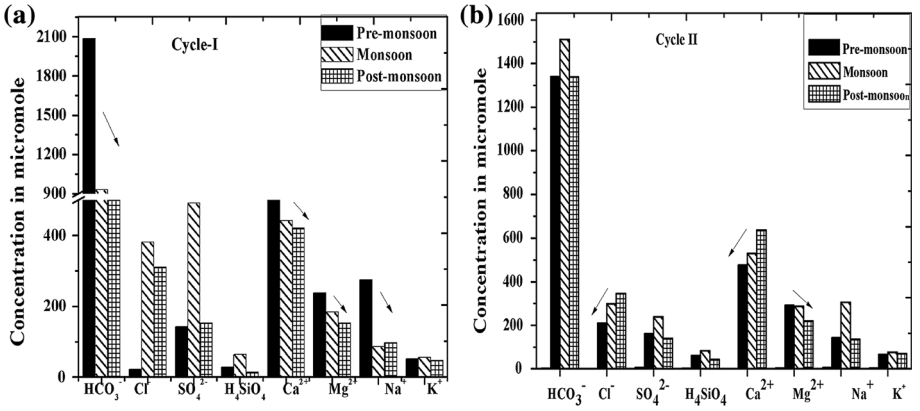

Fig. 2 Temporal change in the major ion concentration of the Brahmaputra River. Pre-monsoon, monsoon and post-monsoon represent the time of sampling event, i.e. **a** cycle I (2011–2012) and **b** cycle II (2013–2014)

found that EC is a good indicator for the chloride. Trends show that low Cl^- concentration in cycle II was due to low EC. Average NO_3^- concentration was high in monsoon season and PO_4^{3-} concentration was high in pre-monsoon season for cycle I and cycle II. Leaching of fertilizers from the agriculture-dominated areas, sewage effluents and decomposition of organic matter are possible source of NO_3^- and PO_4^{3-}.

Average SO_4^{2-} concentration was high in monsoon season for cycle I and cycle II. It was reported that oxidation of pyritic sediments and dissolution of gypsum or anhydrites are major contributor of sulphate in water (Gansser 1964). These processes may add high SO_4^{2-} concentration in water. Other possible anthropogenic sources of SO_4^{2-} are run-off from agricultural land and untreated effluents discharged in the river system. Average H_4SiO_4 content was high in monsoon season. It was reported that high discharge and weathering of igneous and metamorphic rocks contribute higher concentrations of silica (Stallard and Edmond 1981). In general below pH 9 silicon released by weathering as silicic acid (Iler 1979; Krauskopf 1967). The increase in H_4SiO_4 concentration in cycle II indicates increase in intensity of weathering and dissolution of mineral. Therefore, weathering of minerals is the primary source of silica in the freshwater system.

Average Na^+ concentration was found to be high in pre-monsoon season for cycle I and in monsoon for cycle II. Concentration of Na^+ in cycle I and cycle II shows increase in monsoon and post-monsoon seasons. The main source of sodium is the weathering of silicate minerals, halite dissolution and atmospheric precipitation. Average potassium (K^+) concentration was high in monsoon season for cycle I and cycle II. It was found that there was not much variation in K^+ concentration during the three seasons. Major contributions of K^+ are the weathering of rocks and minerals in the catchment. Other possible sources of K^+ are decay of organic matter and springs/groundwater.

Average Ca^{2+} concentration was high in pre-monsoon season for cycle I and post-monsoon season in cycle II. Ca^{2+} shows increase in concentration in next cycle for all three seasons. The main source of Ca^{2+} is carbonate rocks (limestones, dolomite) that are dissolved by carbonic acid contained in water. Average Mg^{2+} concentration was high in pre-monsoon for cycle I and cycle II. There was no significant increase in Mg^{2+} concentration in next cycle. Magnesium in natural water is mainly contributed through ferromagnesian minerals (e.g. olivine, pyroxene and amphiboles) in igneous rocks and magnesium carbonate in sedimentary rocks. The high concentration of Mg in non-monsoon season was due to anthropogenic impact.

The seasonal change in major ions composition during the study period is shown in Fig. 2. Temporal variation of average anion concentration in river water in decreasing order was as follows: $HCO_3^- > SO_4^{2-} > Cl^- > H_4SiO_4 > NO_3^- > PO_4^{3-}$. The abundance of major cations concentration in decreasing order was as follows: $Ca^{2+} > Mg^{2+} > Na^+ > K^+$ in all the seasons. An overall study shows that concentrations of ions were high during pre-monsoon followed by monsoon and post-monsoon seasons. In cycle I (2011–2012), concentration of HCO_3^-, Ca^{2+}, Mg^{2+}, Na^+ and K^+ was high in pre-monsoon season. In cycle II (2013–2014), concentration of Cl^-, SO_4^{2-}, H_4SiO_4, HCO_3^-, Na^+ and K^+ was found to be high in monsoon season. For cycle I, pre-monsoon was dominant, and for cycle II monsoon and post-monsoon were dominant. The high concentration of ion in non-monsoon season was attributed due to anthropogenic impact and in monsoon season was due to influx of run-off, influence through cyclic salts. Considering the maximum land use for agriculture, manures and pesticides are important source of NO_3^- and PO_4^{3-}.

4.2 Atmospheric Supply

4.2.1 Rain Water Correction

The correction for precipitation input and, in case of Na^+, the additional contribution from anthropogenic activities and saline soil were corrected by using the method given in Das et al. (2005):

$$X_{rr} = (X/Cl)r_r x\ Clrr/f_{et} \quad (1)$$

where X_{rr} is the contribution of rain (μM) to rivers; $(X/Cl)_r$ is the molar abundance ratio in rain; Clrr is the concentration of chloride in rain; and f_{et} is the correction factor for evapotranspiration. For the rivers draining into the Bay of Bengal, $f_{et} = 0.6$ has been used, according to Das et al. (2005). The rainwater-corrected concentration (X^*) is calculated as

$$X^* = X_r - X_{rr} \quad (2)$$

where $X = Na^+,\ K^+,\ Ca^{2+},\ Mg^{2+}, SO_4^{2-}$

The contribution of Cl^- and Na^+ (μM) from anthropogenic sources and saline soils to the river can be derived from

$$Cl_s = Cl_r - Cl_{rain}/0.6 \quad (3)$$

$$Na_s = Cl_s$$

$$Na^* = Na_r - (Na_{rr} + Na_s) \quad (4)$$

where Na^* represents precipitation plus anthropogenic and salt-affected saline soil contribution corrected Na^+ concentration, subscripts s and r refer to salt-affected plus anthropogenic sources and river, and 0.6 is the evapotranspiration factor as suggested by Das et al. (2005).

Atmospheric deposition has been considered as a major source of dissolved species in the river water system (Jha et al. 2009; Krishnaswami and Singh 2005). Three major sources of soluble substances in a river were identified by Berner and Berner (1996): (1) sea salts carried in the atmosphere and deposited on the land; (2) weathering reactions taking place in the drainage basin and (3) atmospheric deposition. Cl^- concentration through precipitation is generally used as a parameter for evaluating atmospheric contribution due to conservative behaviour of Cl^- during surface processes (e.g. chemical weathering and hydrological mixing between water resources). MacIntyre (1970) indicated that 90 % of the Cl^- in rivers is derived from the transport of the sea-salt aerosol to the continents and subsequent deposition and run-off from soil. The Cl^- concentration in rainwater at Mohanbari (Dibrugarh) of the Brahmaputra River valley was 20 μM (Subramanian 2004). An atmospheric input correction has been estimated by quantifying and subtracting the portion of the elements derived from rainwater in the chemical composition of the surface water. The correction for the input of dissolved cations and Cl^- from precipitation is determined from the ion/Cl^- ratio (Satsangi et al. 1998). Other possible sources such as saline soil, the influx of groundwater and anthropogenic activities result in high concentrations of Cl^- in river water samples (Kumar et al. 2009a, b; Jha et al. 2009).

4.3 Weathering

Weathering is a natural phenomenon that plays an important role in determining water chemistry. Gibbs plot showed TDS versus weight ratio of (Na + K)/(Na + K + Ca) or Cl/(Cl + HCO_3^-) provides information on three major mechanisms controlling water chemistry (Fig. 3), which include atmospheric precipitation, mineral/rock weathering and evaporation (Gibbs 1970). The Gibbs diagram shows that the most of data fall in the weathering zone except at few samples in the monsoon 2011 and 2013, suggesting that the major mechanism controlling the water chemistry of the Brahmaputra River is the chemical weathering of the rock-forming minerals. Monsoon season of both cycles seems to have differences in terms of cationic input.

Results of major ions ratio of water samples of the Brahmaputra River for pre-monsoon, monsoon and post-monsoon seasons are shown in Table 2. High (Ca^{2+} + Mg^{2+})/Tz^+ ratio with a mean value of 0.91 and 0.96 in the monsoon season for cycle I and cycle II, respectively, reflects the alkaline earth metals released by carbonate weathering (Fig. 4). The high average molar ratio (Ca^{2+} + Mg^{2+})/(Na^+ + K^+), with a maximum value of 4.97 (cycle I) and 3.85 (cycle II) in the post-monsoon season, indicates influence of silicate weathering along with carbonate weathering.

Relatively lower ratio of Ca^{2+} + Mg^{2+})/(Na^+ + K^+) during monsoon season of cycle II due to higher amount of Na^+ and K^+ indicates addition of ions through anthropogenic source, which could be attributed to high run-off. Mean ratio of HCO_3^-/Ca^{2+} + Mg^{2+} suggests significance of silicate weathering controlling the water chemistry of the Brahmaputra River. The molar ratios of Cl^-/Na^+, with a maximum mean value of 16.7 (cycle I) and 0.47 (cycle II) in the post-monsoon season, indicate enrichment of the anion through evaporation. The low molar ratio of Cl^-/Na^+ value (1.40) and (1.01) during non-monsoon season in both cycles indicates the addition of sodium through silicate weathering.

The average ionic ratio of Ca^{2+}/SO_4^{2-} was more than 1 (>1) during the entire monitoring period and cycle, indicating that H_2SO_4 does not replace H_2CO_3 as a source of protons for rock weathering. High average molar ratio of HCO_3^-/H_4SiO_4, i.e. in post-monsoon season

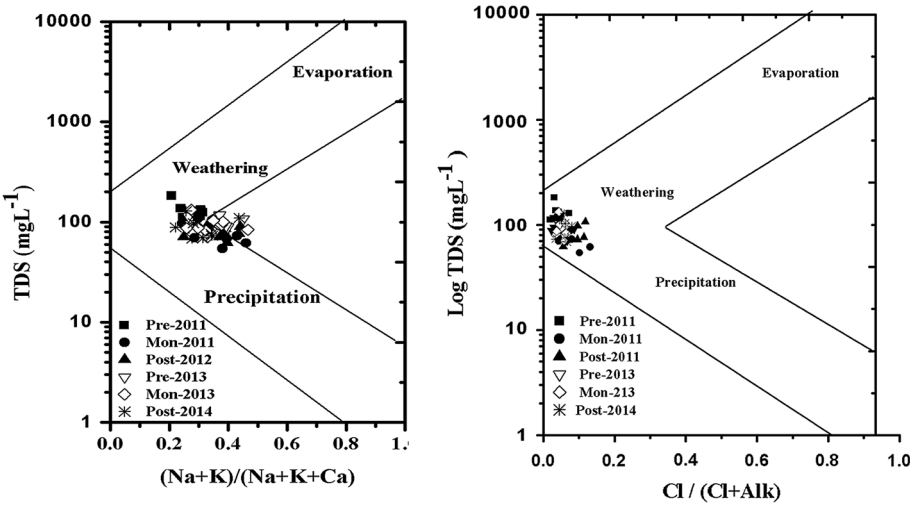

Fig. 3 Gibbs plot depicting the major processes governing water chemistry in different seasons

Table 2 Major ions ratio of the Brahmaputra River water samples for pre-monsoon, monsoon and post-monsoon seasons

	Pre-monsoon		Monsoon		Post-monsoon	
	Range 2011–2012	Range 2013–2014	Range 2011–2012	Range 2013–2014	Range 2011–2012	Range 2013—2014
(*a*)						
$(Ca^{2+}/Na^{+})^{a}$	3.15–5.72	2.27–4.99	1.61–5.46	1.59–5.15	1.76–5.21	2.12–5.80
$(Mg^{2+}/Na^{+})^{a}$	1.09–3.29	0.85–3.11	0.51–1.92	0.94–2.12	0.43–2.25	0.56–1.87
$(HCO_3^{-}/Na^{+})^{a}$	0.48–13.9	3.41–7.56	13.8–31.7	2.85–4.91	2.10–50.3	3.41–6.04
$(Ca^{2+}/Mg^{2+})^{a}$	1.61–2.93	0.73–2.78	1.17–3.19	1.68–4.37	1.06–4.04	2.70–6.10
$(Na^{+} + K^{+})/Tz^{+})^{b}$	0.12–0.21	0.16–0.26	0.17–0.46	0.20–0.30	0.11–0.28	0.17–0.27
$(Ca^{2+} + Mg^{2+})/Tz^{+})^{b}$	0.79–0.88	0.74–0.83	0.78–1.12	0.66–1.43	0.47–0.79	0.56–1.20
$(Cl^{-}/Na^{+})^{b}$	0.28–0.71	0.19–0.54	0.32–0.59	0.26–0.67	0.30–0.61	0.22–0.52
$(HCO_3^{-}/H_4SiO_4)^{c}$	42.8–157	9.02–59.4	10.4–41.9	7.03–35.7	26.1–181	17.6–59.5
$(Ca^{2+} + Mg^{2+})/(Na^{+} + K^{+})^{b}$	3.74–7.55	2.88–5.1	1.90–5.50	2.25–5.13	1.99–5.29	2.31–6.1
$(HCO_3^{-})/(Ca^{2+} + Mg^{2+})^{b}$	1.08–1.28	0.98–1.25	0.80–1.15	0.67–1.41	0.71–1.34	0.72–1.38
$(Ca^{2+}/SO_4^{2-})^{b}$	2.80–5.27	1.70–17.7	1.09–3.25	1.20–5.38	4.00–12.8	2.90–7.15
	Pre-monsoon		Monsoon		Post-monsoon	
	Average 2011–2012	Average 2013–2014	Average 2011–2012	Average 2013–2014	Average 2011–2012	Average 2013–2014
(*b*)						
$(Ca^{2+}/Na^{+})^{a}$	4.07	3.21	2.93	3.40	2.58	3.68
$(Mg^{2+}/Na^{+})^{a}$	1.92	1.64	1.54	1.32	1.18	0.98
$(HCO_3^{-}/Na^{+})^{a}$	7.73	5.42	4.36	4.91	4.01	4.36
$(Ca^{2+}/Mg^{2+})^{a}$	2.24	2.15	2.00	2.65	2.43	3.99
$(Na^{+} + K^{+})/Tz^{+})^{b}$	0.17	0.21	0.27	0.26	0.20	0.21
$(Ca^{2+} + Mg^{2+})/Tz^{b}$	0.83	0.79	0.91	0.96	0.61	0.81
$(Cl^{-}/Na^{+})^{b}$	1.40	0.38	11.0	0.49	16.7	0.38

Table 2 continued

	Pre-monsoon		Monsoon		Post-monsoon	
	Average 2011–2012	Average 2013–2014	Average 2011–2012	Average 2013–2014	Average 2011–2012	Average 2013–2014
$(HCO_3^-/H_4SiO_4)^c$	83.4	30.6	25.6	21.3	92.9	39.9
$(Ca^{2+} + Mg^{2+})/(Na^+ + K^+)^b$	4.97	3.85	3.71	3.71	3.19	3.83
$(HCO_3^-)/(Ca^{2+} + Mg^{2+})^b$	1.18	1.12	0.98	1.05	1.08	0.96
$(Ca^{2+}/SO_4^{2-})^b$	3.71	4.51	1.96	2.99	7.04	4.83

[a] Indicates precipitation-corrected ionic ratio

[b] Indicates ionic ratio

[c] Indicates molar ratio

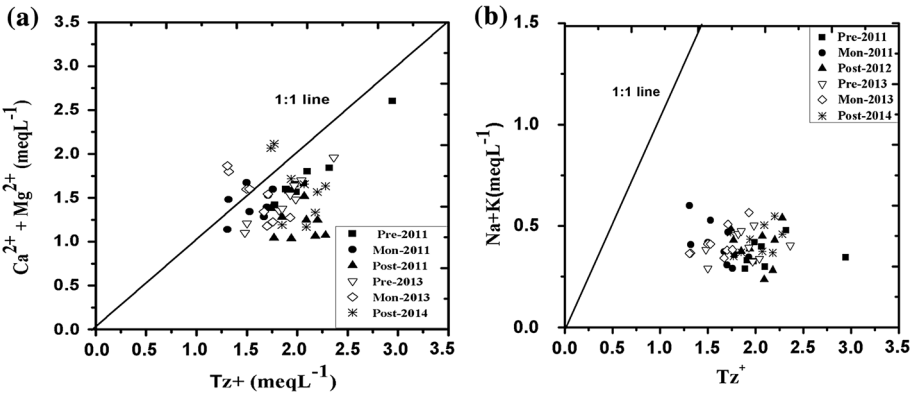

Fig. 4 **a** A plot of $(Ca^{2+} + Mg^{2+})/Tz$ illustrating contribution of alkaline earth element to the total cation charge of the water during different seasons. **b** A plot of $(Na^{+} + K^{+})/Tz^{+}$ illustrating contribution of alkali ions to the total cation of the water in different seasons

for cycle I (92.9) and cycle II (32.9), indicated contribution of ions from non-silicate source. The plot of $(Ca^{2+} + Mg^{2+})$ versus Tz^{+} (Fig. 4a) for the samples shows that most of the points lie below the equiline indicating the contribution from carbonate weathering in the catchment area. The average ratio of $(Na^{+} + K^{+})/Tz^{+}$ shows maximum value of 0.18 in pre-monsoon season of 2011–2012 and 0.21 in monsoon season of 2013–2014.

A cross-plot of $(Na^{+} + K^{+})/Tz^{+}$ suggests input from silicate weathering along with anthropogenic activities (Fig. 4b). Contribution of Na + K to the total cation (Tz^{+}) was high in the monsoon of 2011 and 2013 indicating input from anthropogenic source. The dissolution of various potassium minerals, namely feldspars (orthoclase and microcline) and the weathering of the chlorine minerals carnallite and sylvite, could be the source of potassium in water. High contribution of (Ca + Mg) to the total cation (Tz^{+}) and low ratios of $(Na + K)/Tz^{+}$ in both cycles indicate that contribution of dissolved ions in the Brahmaputra River was carbonate weathering with little contribution from silicate weathering. It was reported that carbonate weathering contributes half of the dissolved solids in rivers in the global scale (Meybeck 1983; Singh et al. 2005).

The ratios of Ca^{2+}/Na^{+} and Mg^{2+}/Na^{+} are used to calculate relative proportions of Ca^{2+} and Mg^{2+} ions derived from carbonate weathering and silicate weathering (Hren et al. 2007). Mean ratio of Ca^{2+}/Na^{+} was maximum in pre-monsoon for cycle I and in post-monsoon for cycle II. Mean ratio of Mg^{2+}/Na^{+} was maximum in pre-monsoon season in both cycles. These higher ratios indicated the dominance of Ca^{2+} and Mg^{2+} over Na^{+} in weathering of mafic minerals and dissolution of carbonate minerals. High mean ratio of Ca^{2+}/Na^{+} during post-monsoon and Mg^{2+}/Na^{+} during pre-monsoon suggests either an enrichment of Ca^{2+} and Mg^{2+} or depletion in Na^{+}. Average mean ratio of Ca^{2+}/Mg^{2+} was found to be high during post-monsoon season for cycle I and cycle II. Lower mean ratio value of Ca^{2+}/Mg^{2+} as compared to global mean of 2.40 during pre-monsoon suggested weathering of Mg^{2+} rich minerals. High ratio of Ca^{2+}/Mg^{2+} during post-monsoon indicated incongruent dissolution of carbonate minerals.

Precipitation-corrected molar ratio plot for (Mg^{2+}/Na^{+}) versus (Ca^{2+}/Na^{+}) and (HCO_3^{-}/Na^{+}) versus (Ca^{2+}/Na^{+}) for different seasons is shown in Fig. 5. Silicate and carbonate are the two end members for the precipitation-corrected molar ratios. It was found that most of the samples fall between the silicate end member (granites) and carbonate end member which indicates the combined effect of silicate weathering and

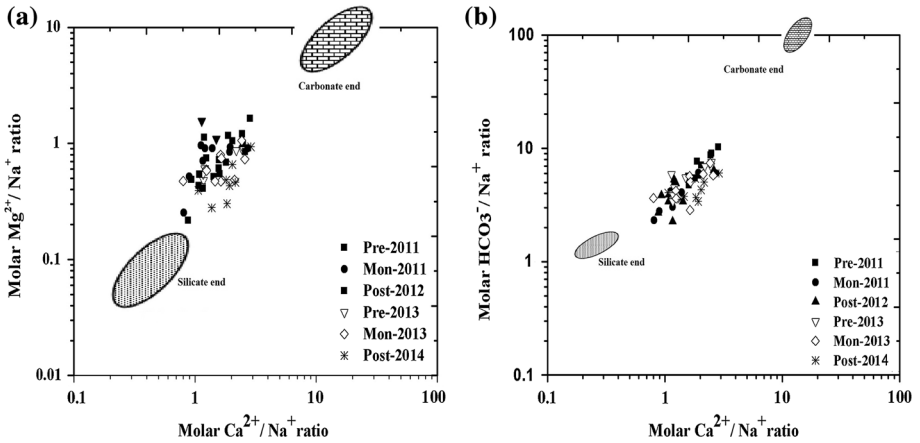

Fig. 5 Precipitation-corrected molar ratio plot for **a** (Mg^{2+}/Na^{+}) versus (Ca^{2+}/Na^{+}) and **b** (HCO_3^{-}/Na^{+}) versus (Ca^{2+}/Na^{+}) for different seasons. Patches show end member of granite silicate (lower *circle filled black*) and carbonate (upper *circle with brick legends*)

dissolution of carbonate rocks. However, with different compositions during different seasons there was shift in samples from silicate end to carbonate end. Post-monsoon 2014 and monsoon 2011 showed clustering, but there was shift towards carbonate end from monsoon 2013 to post-monsoon 2014.

4.4 Statistical Analysis

4.4.1 Analysis of Variance (ANOVA)

ANOVA was performed for each parameter to check among the parameters for various seasons during 2011–2012 and 2013–2014. The results of ANOVA are given in Table 3. In

Table 3 Results of analysis of variance (ANOVA) of each parameter for pre-monsoon, monsoon and post-monsoon seasons during 2011–2012 and 2013–2014

Parameter	Cycle I (2011–2012)		Cycle II (2013–2014)	
	Fcritical	Fcalculated	Fcritical	Fcalculated
pH	3.40	**4.09**	3.40	**4.18**
EC	3.40	**25.0**	3.40	0.54
TDS	3.40	**25.0**	3.40	0.58
HCO_3^{-}	3.40	**23.0**	3.40	0.58
Cl^{-}	3.40	0.88	3.40	2.97
SO_4^{2-}	3.40	**19.9**	3.40	2.58
NO_3^{-}	3.40	2.21	3.40	1.97
PO_4^{3-}	3.40	0.55	3.40	1.97
H_4SiO_4	3.40	**16.3**	3.40	**5.72**
Na^{+}	3.40	0.91	3.40	0.42
k^{+}	3.40	**3.61**	3.40	0.74
Ca^{2+}	3.40	**9.74**	3.40	2.81
Mg^{2+}	3.40	**4.57**	3.40	**4.25**

Bold indicates Fcritical > Fcalculated

cycle I, all the parameters exhibit significant variation except NO_3^-, PO_4^{3-}, Cl^- and Na^+ which indicates significant seasonal variations owing to contributions from weathering processes. In cycle II, pH, H_4SiO_4 and Mg^{2+} show significant temporal change which indicates input of freshwater in monsoon season and change in pH may cause variation in H_4SiO_4 and Mg^{2+} concentration. Anthropogenic impacts seem to be suppressed as in case with NO_3^- and PO_4^{3-}. Increase in $F_{calculated}$ value in case of pH, HCO_3^-, Cl^- and Ca^{2+} in cycle II indicates significant cyclic change, which may be due to influx of run-off and weathering process.

4.4.2 Principal Component Analysis (PCA)

Table 4 shows the result of factor analysis of water samples, for three seasons, i.e. pre-monsoon, monsoon and post-monsoon seasons. The variables present in the factors for three seasons are pH, EC, HCO_3^- Cl^-, NO_3^-, PO_4^{3-}, SO_4^{2-}, H_4SiO_4, Na^+, K^+, Ca^{2+} and Mg^{2+}. Factor 1 accounts for 22.7 % variance. The dominant factors are EC, TDS, HCO_3^- and Ca^{2+} which indicates that weathering is the dominant process and release of HCO_3^- during carbonate weathering. Factor 2 accounts for 15.6 % variance. The variables are PO_4^{3-}, $H_4SiO_4^-$ and K^+ contribution of ion through anthropogenic source such as anthropogenic activities such as agricultural run-off in the catchment area. Factor 3 accounts for 12.0 %, and variables are Na^+ and Cl^- which indicates enrichment of salt through atmospheric precipitation. Factor 4 accounts for 9.87 %, and variables are NO_3^- which indicates nutrient enrichment mainly because of heavy irrigation and fertilizer additive used to cultivate vegetables and other agriculture products and on background carbonate weathering continuous to operate.

Table 4 Factor analysis of water samples of the Brahmaputra River for pre-monsoon, monsoon and post-monsoon seasons

	Factors			
	F1	F2	F3	F4
Rotated component matrix				
Ph	0.272	−0.280	−0.141	0.496
EC	0.**890**	0.036	0.100	−0.027
TDS	0.**890**	0.036	0.101	−0.027
HCO_3^-	0.**712**	−0.018	−0.132	−0.043
Cl^-	0.074	−0.176	0.**801**	−0.095
SO_4^{2-}	0.164	0.316	0.217	−0.152
NO_3^-	0.055	−0.123	−0.057	0.**669**
PO_4^{3-}	0.056	0.**767**	0.048	−0.068
H_4SiO_4	−.095	0.**724**	−.020	−0.080
Na^+	−0.077	0.108	0.**826**	0.079
K^+	0.261	0.**730**	−0.269	0.147
Ca^{2+}	0.**765**	0.203	−0.037	0.202
Mg^{2+}	0.287	−0.318	−.223	−0.**689**
Eigen value	2.96	2.03	1.56	1.28
% of variance	22.7	15.6	12.0	9.87
CV	22.7	38.3	50.3	60.2

Bold indicate significant loading

The factor score was estimated to find out the spatial variation of the factor representation and to identify the zone of its representation. They are commonly obtained by two approaches: weighted least square method and the regression method. The regression method is used in the study to compute the factor scores. The higher the factor scores, the higher the factor's influence (Felipe-Sotelo et al. 2007; Bu et al. 2010). The factor score plot for first two factors pre-monsoon, monsoon and post-monsoon is shown in Fig. 6. In pre-monsoon season, high factor score 1 is observed at sampling locations B4, B5, B8 and B9 which are representative of carbonate weathering and bicarbonate. Similarly, high factor score 2 is observed at sampling

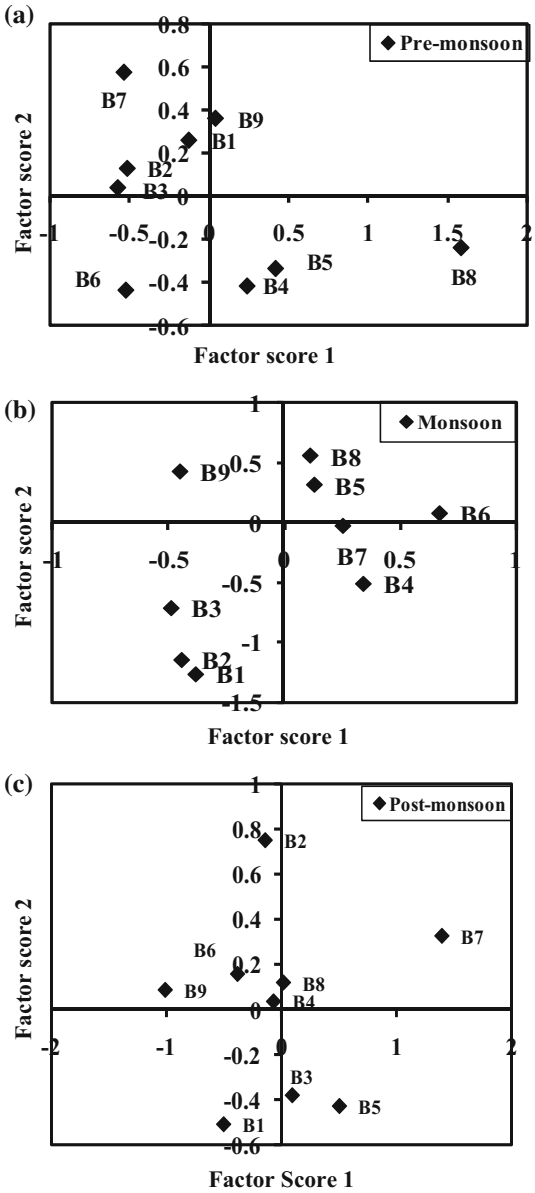

Fig. 6 Factor score plot of factor 1 and factor 2 for **a** pre-monsoon, **b** monsoon and **c** post-monsoon seasons

locations B1, B2, B3, B7 and B9 which were likely polluted by industrial waste and agriculture run-off. In monsoon season, factor scores 1 and 2 are observed for high B5, B6, B8 and B9 which indicate influx of run-off. In post-monsoon season, high factor score 1 is observed at sampling locations B4, B5, B7 and B9 which are representative of silicate weathering. Similarly, high factor score 2 in post-monsoon season is observed at sampling locations B7, B8 and B9 which were likely polluted by anthropogenic input. Using factor score, it has been observed that at downstream location pollution is more pronounced as compared to upstream. In relation to the sampling seasons, high factor score 1 is observed at pre-monsoon season and factor score 2 at post-monsoon season infers that impact is less pronounced during monsoon season due to dilution effect by rainfall.

4.5 Effective CO_2 Pressure

The partial pressure of CO_2 (P_{CO_2}) in streams and rivers reflects both internal carbon dynamics and external biogeochemical processes in terrestrial ecosystems (Jones et al. 2003). As carbonate weathers, alkalinity is generated leading to an increase in pH and a reduction in P_{CO_2}. The effective CO_2 pressure ($\log P_{CO_2}$) for pre-monsoon, monsoon and post-monsoon samples of the Brahmaputra River has been estimated from pH values and HCO_3^- concentration (Table 5). In the year 2011–2012, average P_{CO_2} values were found to be $10^{-2.4}$ in pre-monsoon, $10^{-2.9}$ in monsoon and $10^{-3.2}$ in post-monsoon. In the year 2013–2014, average P_{CO_2} values were found to be $10^{-3.1}$ in pre-monsoon, $10^{-2.6}$ in monsoon and $10^{-2.5}$ in post-monsoon which are higher than the atmospheric value, i.e. $10^{-3.5}$. This follows the global trend of river water showing disequilibrium with the atmosphere (Garrels and Mackenzie, 1971). This may be due to the contribution of groundwater containing high CO_2, the slow rate of its re-equilibrium between surface water and the atmosphere by release of excess CO_2 (Subramanian et al. 2006; Sharma and Subramanian 2008; Jha et al. 2009). High P_{CO_2} values are likely to arise from the coupling of sulphide oxidation and carbonate dissolution (Wadham et al. 1998).

4.6 Chemical Weathering Rates

The weathering rates (carbonate and silicate) are calculated using TDS and run-off values (mm $year^{-1}$) which are shown in Table 6. The run-off data (879 mm $year^{-1}$) for the Brahmaputra River were taken from Gaillardet et al. (1999). As shown in Table 6(a), SWR in cycle I and cycle II was found to be high in monsoon season and maximum at B9. As shown in Table 6(b), CWR in cycle I and cycle II was found to be high in pre-monsoon season. As compared with previous findings, average annual SWR was found to be lower than the value found by Gaillardet et al. (1999), whereas average CWR was found to be higher than previous reported value. Rapid rock uplift and different physical erosion rates are responsible for high CWR. In the Brahmaputra River, run-off and relief are the factors that control physical erosion which in turn controls the chemical erosion by increasing specific surface area for chemical reaction (Gupta 2008).

4.7 CO_2 Consumption Rates

The Brahmaputra River basin is the fifth largest river basin in the world and transports significant amounts of all physically and chemically weathered material from the catchment area. Therefore, it is important to determine the CO_2 consumption rate of this river.

Table 5 Log$mHCO_3^-$ and logP_{CO_2} values for pre-monsoon, monsoon and post-monsoon samples

Sites	Pre-monsoon		Monsoon		Post-monsoon	
	Log $mHCO_3^-$	Log P_{CO_2}	Log $mHCO_3^-$	Log P_{CO_2}	Log mHO_3^-	Log P_{CO_2}
2011–2012						
B-1	−2.71	−1.30	−2.83	−2.99	−2.81	−3.01
B-2	−2.69	−2.69	−2.76	−2.72	−2.94	−2.48
B-3	−2.76	−2.51	−2.86	−2.99	−2.88	−2.45
B-4	−2.67	−2.48	−2.83	−2.54	−2.83	−2.50
B-5	−2.64	−3.09	−2.91	−1.50	−2.86	−2.66
B-6	−2.72	−3.33	−2.91	−2.59	−2.94	−2.56
B-7	−2.74	−3.74	−2.83	−2.75	−3.01	−2.14
B-8	−2.53	−2.78	−2.88	−2.96	−2.88	−2.46
B-9	−2.76	−2.50	−2.88	−2.51	−2.92	−2.66
Avg ± SD	−2.69 ± 0.07	−2.71 ± 0.68	−2.86 ± 0.05	−2.62 ± 0.46	−2.90 ± 0.06	−2.55 ± 0.23
2013–2014						
B-1	−2.65	−2.95	−2.81	−2.91	−2.94	−3.44
B-2	−2.88	−2.31	−2.74	−2.58	−2.79	−2.26
B-3	−2.76	−2.02	−2.87	−2.99	−2.86	−3.56
B-4	−2.74	−2.26	−2.81	−2.54	−2.78	−3.27
B-5	−2.94	−2.37	−2.82	−1.50	−2.78	−3.13
B-6	−3.39	−2.60	−2.71	−2.59	−2.91	−2.76
B-7	−3.79	−3.02	−2.78	−2.75	−2.71	−2.54
B-8	−2.78	−2.61	−3.09	−2.96	−2.88	−2.81
B-9	−2.75	−2.59	−2.74	−2.58	−2.81	−2.66
Avg ± SD	2.97 ± 0.37	2.53 ± 0.32	−2.82 ± 0.11	−2.60 ± 0.45	−2.83 ± 0.07	−2.94 ± 0.44

Table 6 Chemical weathering rate (CWR) for the Brahmaputra River for pre-monsoon, monsoon and post-monsoon during (a) silicate weathering rate (SWR) and (b) carbonate weathering rate (CWR) for 2011–2012 (cycle I) and 2013–2014 (cycle II)

I.D.	Silicate weathering rate (SWR)					
	Pre-monsoon		Monsoon		Post-monsoon	
	SWR tkm^{-2} $year^{-1}$ 2011–2012	SWR $tkm^{-2}year^{-1}$ 2013–2014	SWR $tKm^{-2}year^{-1}$ 2011–2012	SWR $tKm^{-2}year^{-1}$ 2013–2014	SWR $tKm^{-2}year^{-1}$ 2011–2012	SWR $tKm^{-2}year^{-1}$ 2013–2014
(*a*)						
B1	8.70	6.72	5.94	3.97	3.99	2.54
B2	8.59	6.97	8.53	6.91	3.16	1.71
B3	3.41	4.98	2.58	3.03	1.33	1.38
B4	4.05	2.69	11.0	9.66	9.67	8.39
B5	8.42	6.89	8.34	6.62	11.2	9.41
B6	9.76	7.23	11.9	8.75	0.004	1.77
B7	4.56	3.54	6.01	4.56	5.72	3.93
B8	5.00	3.55	7.93	5.95	3.72	1.12
B9	6.00	4.79	15.1	13.64	5.71	4.35
Range	3.41–9.75	2.69–7.23	2.58–15.1	3.03–13.6	0.004–11.2	1.12–9.41
Avg ± SD	6.5 ± 2.38	5.29 ± 1.71	8.59 ± 3.69	7.01 ± 3.9	4.94 ± 2.94	3.85 ± 3.08
I.D.	Carbonate weathering rate (CWR)					
	Pre-monsoon		Monsoon		Post-monsoon	
	CWR tkm^{-2} $year^{-1}$ 2011–2012	CWR tkm^{-2} $year^{-1}$ 2013–2014	CWR tKm^{-2} y^{-1} 2011–2012	CWR tKm^{-2} $year^{-1}$ 2013–2014	CWR tKm^{-2} $year^{-1}$ 2011–2012	CWR tKm^{-2} $year^{-1}$ 2013–2014
(*b*)						
B1	92.9	74.0	63.4	57.4	64.0	60.0
B2	96.4	77.1	77.4	68.9	53.0	49.8

Table 6 continued

I.D.	Carbonate weathering rate (CWR)					
	Pre-monsoon		Monsoon		Post-monsoon	
	CWR tkm^{-2} $year^{-1}$ 2011–2012	CWR tkm^{-2} $year^{-1}$ 2013–2014	CWR tKm^{-2} y^{-1} 2011–2012	CWR tKm^{-2} $year^{-1}$ 2013–2014	CWR tKm^{-2} $year^{-1}$ 2011–2012	CWR tKm^{-2} $year^{-1}$ 2013–2014
B3	80.3	24.6	60.2	26.2	53.0	18.8
B4	99.2	83.6	68.1	57.1	64.4	54.7
B5	108	87.2	63.2	54.9	60.3	49.1
B6	94.2	24.6	62.0	26.2	46.4	18.8
B7	88.5	92.9	69.5	55.9	51.9	52.7
B8	138.3	117	66.8	58.9	62.2	58.5
B9	81.9	66.6	66.9	51.8	51.9	46.2
Range	80.3–138	24.6–117	60.2–77.4	26.2–68.9	46.4–64.4	18.8–60.0
Avg ± SD	97.7 ± 17.4	77.4 ± 24.7	66.4 ± 5.14	55.0 ± 11.9	56.3 ± 6.47	48.5 ± 12.2

Run-off value: 879 million $year^{-1} \times 10^6$ (Gaillardet et al. (1999), 840 million $year^{-1} \times 10^6$ (2011), 640 million $year^{-1} \times 10^{6\ (2012),\ 570}$ million $year^{-1} \times 10^6$ (2013), 581 (2014) (Central Water Commission)

Based on major ion composition of the water samples, CO_2 consumption rate of the Brahmaputra River has been calculated by using the following formulae given by the Jha et al. (2009) and Wu et al. (2008).

4.7.1 CO_2 Consumption Rate

$$[\Phi CO_2]_{Sil} = \Phi(Tz+)_{sil} = (2Ca_{sil} + 2Mg_{sil} + Na_{sil} + K_{sil}) \times \text{discharge/drainage area.} \quad (5)$$

$$[\Phi\ CO_2]_{Carb} = \Phi\,(Tz+)_{carb} = (Ca_{carb} + Mg_{carb}) \times \text{discharge/drainage area.} \quad (6)$$

where Ca_{sil}, Mg_{sil}, Na_{sil} and K_{sil} represent cation released by the silicate weathering and Ca_{carb}, and Mg_{carb} represent Ca and Mg supplied from carbonate weathering.

4.7.2 Silicate Weathering Rate

Silicate weathering is an important source of major ions to river. The proportions of silicate and carbonate weathering on the earth's surface are important in long-term global CO_2 balances (Berner et al. 1983). In the present study, Cl^- was used as an index to derive silicate component of Na in calculating CO_2 consumption rate. Silicate and carbonate weathering rates in the Brahmaputra River are calculated using cation components supplied from silicate and carbonate, coupled with discharge per unit area.

The silicate weathering rate (SWR) is calculated as proposed by Roy et al. 1999

$$SWR = (Ca_{sil} + Mg_{sil} + Na_{sil} + K_{sil} + SiO_2) \times \text{discharge/drainage area} \quad (7)$$

where Ca_{sil}, Mg_{sil}, Na_{sil} and K_{sil} represent cations supplied by silicates (mg L^{-1})

The carbonate weathering rate (CWR) is calculated as per Roy et al. 1999

$$CWR = \left[Ca_{carb} + Mg_{carb} + 0.5 \times \left(HCO_3^-\right)_{carb}\right] \times \text{discharge/drainage area} \quad (8)$$

Silicate component of major cations

$$Na_{sil} = Na_r - Cl_r \quad (9)$$

$$K_{sil} = K_r - K_{rr}$$

$$Ca_{sil} = Na_{sil} \times (Ca/Na)_{sol}$$

$$Mg_{sil} = Na_{sil} \times (Mg/Na)_{sol}$$

where the subscripts sil, r and sol are silicates, river and solution, respectively. Krr is contribution of K from rain to the river water. (Ca/Na) sol and (Mg/Na) sol are the molar ratios released to river water from silicates in the drainage basins during chemical weathering.

4.7.3 Carbonate Component

$$Ca_{carb} = Ca_r - Ca_{sil} \quad (10)$$

$$Mg_{carb} = Mg_r - Mg_{sil}$$

where the subscripts carb, r and sil are carbonates, river and silicates, respectively

The CO_2 consumption rate due to silicate weathering (W_{Sil}–CO_2) and carbonate weathering (W_{Carb}–CO_2) of the Brahmaputra River for cycle I is shown in Table 7. W_{Sil}–CO_2 shows an average value of 0.31 ($\times 10^6$ mol Km^{-2} $year^{-1}$) in pre-monsoon, 0.70 ($\times 10^6$ mol Km^{-2} $year^{-1}$) in monsoon and 0.44 ($\times 10^6$ mol Km^{-2} $year^{-1}$) in post-monsoon seasons. Average W_{sil}–CO_2 was found to be high in monsoon season and maximum at

Table 7 CO_2 consumption rate due to silicate weathering (W_{Sil}–CO_2) and carbonate weathering (W_{Carb}–CO_2) for the Brahmaputra River for pre-monsoon, monsoon and post-monsoon: (a) cycle I (2011–2012) and (b) cycle II (2013–2014)

Sites	Cycle I (2011–2012)					
	Pre-monsoon		Monsoon		Post-monsoon	
	W_{Sil}–CO_2	W_{Carb}–CO_2	W_{Sil}–CO_2	W_{Carb}–CO_2	W_{Sil}–CO_2	W_{Carb}–CO_2
(*a*)						
B1	0.49	0.55	0.66	0.50	0.41	0.50
B2	0.34	0.63	0.43	0.63	0.40	0.51
B3	0.16	0.21	0.18	0.25	0.17	0.14
B4	0.25	0.74	0.62	0.54	0.68	0.43
B5	0.47	0.70	0.74	0.60	0.50	0.34
B6	0.28	0.63	0.84	0.39	0.41	0.29
B7	0.22	0.69	0.92	0.67	0.47	0.51
B8	0.28	1.08	0.84	0.65	0.40	0.60
B9	0.30	0.56	1.05	0.47	0.52	0.42
Range	0.16–0.49	0.21–1.08	0.18–1.05	0.25–0.67	0.17–0,.68	0.14–0.60
Avg ± SD	0.31 ± 0.11	0.64 ± 0.23	0.70 ± 0.26	0.52 ± 0.13	0.44 ± 0.13	0.42 ± 0.14
Sites	Cycle II (2013–2014)					
	Pre-monsoon		Monsoon		Post-monsoon	
	W_{Sil}–CO_2	W_{Carb}–CO_2	W_{Sil}–CO_2	W_{carb}–CO_2	W_{sil}–CO_2	W_{carb}–CO_2
(*b*)						
B1	0.57	0.67	0.66	0.53	0.42	0.46
B2	0.38	0.50	0.62	0.40	0.49	0.43
B3	0.20	0.16	0.20	0.20	0.19	0.22
B4	0.30	0.64	0.56	0.71	0.77	0.53
B5	0.58	0.49	0.75	0.60	0.41	0.86
B6	0.21	0.34	0.50	0.51	0.42	0.44
B7	0.27	0.42	0.89	0.65	0.54	0.78
B8	0.29	0.61	0.85	0.48	0.46	0.63
B9	0.28	0.69	0.96	0.63	0.58	0.51
Range	0.20–0.58	0.16–0.69	0.20–0.96	0.20–0.71	0.19–0.77	0.22–0.86
Avg ± SD	0.34 ± 0.14	0.50 ± 0.17	0.66 ± 0.23	0.52 ± 0.15	0.48 ± 0.16	0.54 ± 0.19

B4 and B8. The CO_2 consumption rate due to carbonate weathering of the Brahmaputra River for cycle I shows an average value of 0.64 ($\times 10^6$ mol Km^{-2} $year^{-1}$) in pre-monsoon, 0.52 ($\times 10^6$ mol Km^{-2} $year^{-1}$) in monsoon and 0.42 ($\times 10^6$ mol Km^{-2} $year^{-1}$) in post-monsoon seasons. Wcarb–CO_2 was found dominant in pre-monsoon season. However, in monsoon and post-season W_{sil}–CO_2 was dominant which may be due to monsoonal effect.

CO_2 consumption due to silicate weathering for cycle II is presented in Table 7(a). In cycle II, W_{sil}–CO_2 shows an average value of 0.34 ($\times 10^6$ mol Km^{-2} $year^{-1}$) in pre-monsoon, 0.66 ($\times 10^6$ mol Km^{-2} $year^{-1}$) in monsoon and 0.48 ($\times 10^6$ mol Km^{-2} $year^{-1}$) in post-monsoon. Average W_{sil}–CO_2 was found to be high in monsoon season for cycle II. In cycle II, average W_{sil}–CO_2 in pre-monsoon and post-monsoon seasons is higher than cycle I. In Table 7(b) the CO_2 consumption rate due to carbonate weathering (Wcarb–CO_2) of the Brahmaputra River in cycle II shows an average value of 0.50×10^6 mol Km^{-2} $year^{-1}$) in pre-monsoon, 0.52 ($\times 10^6$ mol Km^{-2} $year^{-1}$) in monsoon and 0.54 ($\times 10^6$ mol Km^{-2} $year^{-1}$) in post-monsoon. For cycle II, Wcarb–CO_2 was dominant in pre-monsoon and post-monsoon seasons.

The CO_2 consumption rate associated with total chemical weathering (WChe–CO_2) is presented in Table 8. In cycle I, total CO_2 consumption rate associated with chemical weathering in the Brahmaputra River shows an average value of 0.84 ($\times 10^6$ mol Km^{-2} $year^{-1}$) in pre-monsoon, 1.19 ($\times 10^6$ mol Km^{-2} $year^{-1}$) in monsoon and 1.01 ($\times 10^6$ mol Km^{-2} $year^{-1}$) in post-monsoon. In cycle II, average annual CO_2 consumption rate due to chemical weathering in the Brahmaputra River was found to be 0.99 ($\times 10^6$ mol Km^{-2} $year^{-1}$) in pre-monsoon, 1.28 ($\times 10^6$ mol Km^{-2} $year^{-1}$) in monsoon and 0.95 ($\times 10^6$ mol Km^{-2} $year^{-1}$) in post-monsoon. In both cycles, CO_2 consumption due to chemical weathering was found to be high in monsoon season.

Table 8 CO_2 consumption rate due to chemical weathering (W_{chem} = carbonate + silicate weathering) in different for cycle I and cycle II

	Cycle I & Cycle II					
	Pre-monsoon		Monsoon		Post-monsoon	
	W_{Che}–CO_2	W_{Che}–CO_2	W_{Che}–CO_2	W_{Che}–CO_2	W_{Che}–CO_2	W_{Che}–CO_2
Sites	2011–2012	2013–2014	2011–2012	2013–2014	2011–2012	2013–2014
B1	1.04	1.24	1.16	1.19	0.91	0.87
B2	0.97	0.88	1.06	1.02	0.91	0.92
B3	0.37	0.66	0.40	0.96	0.41	0.85
B4	0.98	0.94	1.16	1.27	1.11	1.30
B5	1.17	1.07	1.33	1.34	0.85	1.27
B6	0.55	0.95	1.00	1.28	0.85	0.96
B7	0.91	0.68	1.59	1.54	0.99	1.32
B8	1.36	0.90	1.49	1.33	1.00	1.09
B9	0.86	0.97	1.51	1.58	0.94	1.09
Range	0.37–1.24	0.66–1.36	0.40–1.58	0.96–1.59	0.41–1.32	0.85–1.11
Avg ± SD	0.84 ± 0.27	0.99 ± 0.19	1.19 ± 0.35	1.28 ± 0.22	1.01 ± 0.29	0.95 ± 0.08

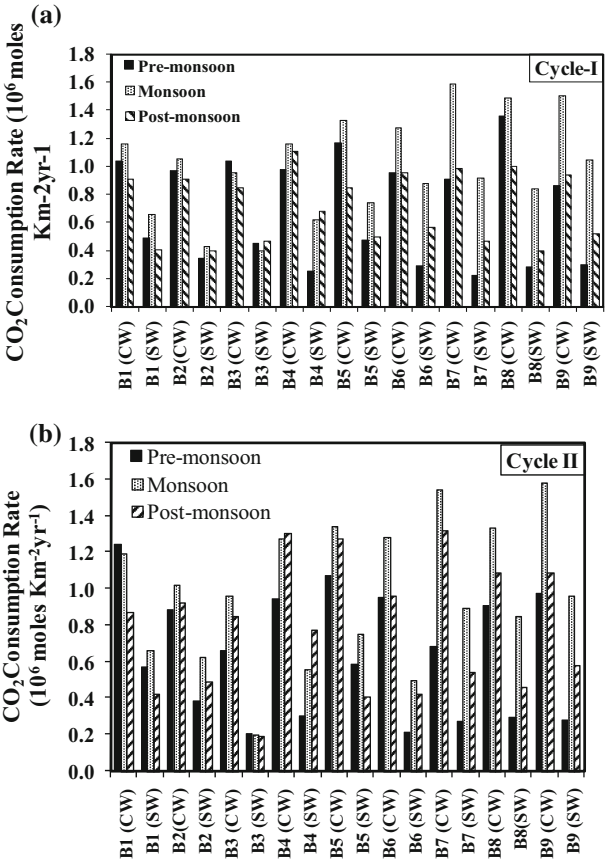

Fig. 7 Atmospheric carbon dioxide (CO_2) consumption rates of the Brahmaputra River at different locations for **a** 2011–2012 (cycle I) and **b** 2013–2014 (cycle II). CW and SW stand for chemical weathering and silicate weathering, respectively

Figure 7a, b shows CO_2 consumption rates of the Brahmaputra River at different locations for cycle I and cycle II. In cycles I and II, all sampling locations except B4 show similar trend for SW (CO_2 consumption due to silicate weathering), i.e. high CO_2 consumption rate in monsoon season. CW (CO_2 consumption due to chemical weathering) for cycle I and cycle II shows similar trend at B3 and B1, i.e. high CW in pre-monsoon season. In post-monsoon season CW was highest at B4. In most of the locations, high SW and CW were found in monsoon season.

From the value of TDS flux and CO_2 consumption of the world's major rivers (Table 9), it was observed that TDS flux of the Brahmaputra River was found to be higher than the Indus River (Himalayan river), the Yellow (Tibetan river) and the Amazon (Global river). The present result showed that TDS yield was lower than that of the major Indian rivers (Ganga, Godavari and Krishna) and other non-Indian rivers like Mekong and the Amazon, but higher than that of the Indus, the Yellow River.

The average annual CO_2 consumption rate due to silicate weathering was found to be 0.52 ($\times 10^6$ mol Km^{-2} $year^{-1}$) and 0.49 ($\times 10^6$ mol Km^{-2} $year^{-1}$) for cycle I and cycle II, respectively. CO_2 consumption rate in the present study was significantly higher than in the previous studies on the Brahmaputra River. Gaillardet et al. 1999 0.15 ($\times 10^6$ - mol Km^{-2} $year^{-1}$, Hren et al. 2007 (0.3×10^6) and lower than Singh et al. 2006

Table 9 TDS flux and CO_2 consumption of the Brahmaputra River and other major rivers of the world

Rivers	TDS flux (tkm^2 $year^{-1}$)	W_{Sil}–CO_2	W_{Carb}–CO_2	References
Brahmaputra	57	0.52	0.55	Present study
Brahmaputra	26	0.49	0.52	
Ganges	171	0.45	0.24	Gaillardet et al. (1999)
Indus	10	0.06	0.09	
Godavari	102	0.29	NA	Jha et al. (2009)
Krishna	28	0.36	NA	Das et al. (2005)
Huang He	NA	0.09	0.27	Wu et al. (2008)
Amazon	147	0.05	0.11	Gaillardet et al. (1999)
Mekong	56	0.28	0.58	
Ganga	72	0.38	NA	Singh et al. (2005)
Indus	42	0.06	NA	
Mekong	72	0.24	NA	
Yellow	25	0.08	NA	
Amazon	35	0.05	NA	
World average	36	0.09	NA	

W_{Carb}–CO_2—(carbonate weathering $\times 10^6$ mol Km^{-2} $year^{-1}$)

WSil–CO_2—(silicate weathering $\times 10^6$ mol Km^{-2} $year^{-1}$)

NA Not available

(0.6×10^6) and other Himalayan rivers, i.e. Ganga 0.38 ($\times 10^6$ mol Km^{-2} $year^{-1}$), Indus 0.06 ($\times 10^6$ mol Km^{-2} $year^{-1}$), and Deccan Trap rivers, i.e. Godavari River 0.29 ($\times 10^6$ mol Km^{-2} $year^{-1}$) and Krishna River 0.36 ($\times 10^6$ mol Km^{-2} $year^{-1}$) and a river like Amazon 0.05 ($\times 10^6$ mol Km^{-2} $year^{-1}$) indicated more intense CO_2 consumption in the Brahmaputra River associated with silicate weathering.

Average CO_2 consumption rate due to carbonate weathering of the Brahmaputra River was found to be 0.55 and 0.52 ($\times 10^6$ mol Km^{-2} $year^{-1}$) for cycle I and cycle II, respectively, which indicates an increase value of (0.01×10^6 mol Km^{-2} $year^{-1}$). As compared with world's major rivers, the CO_2 consumption rate due to carbonate weathering of the Brahmaputra River was found to be higher than that of the Ganga, Indus, Amazon, Huang He and lower than the Mekong River. Our result shows that high CO_2 consumption rate was associated with carbonate weathering.

5 Conclusion

The spatial and temporal variation of major ions during pre-monsoon, monsoon and post-monsoon seasons of 2011–2014 has been carried out by analysing 27 samples (nine samples in each season) from upstream to downstream of the Brahmaputra River. A systematic monitoring of the Brahmaputra River was carried out for 2 years (2011–2014) to determine the weathering and associated CO_2 consumption rates of the Brahmaputra River that could alter the global climate. Estimation of chemical weathering rates of the river indicated that carbonate weathering largely dominates the chemistry of the river water. Atmospheric deposition and anthropogenic activity contributed to major ions and

associated CO_2 consumption. The important findings of this study can be summarized as follows

1. The results indicate that Brahmaputra River waters are neutral to alkaline in nature. EC and TDS values were high in pre- and post-monsoon seasons due to mixing of run-off water which carries larger quantity of salts from catchment area. Concentrations of ions were higher during pre-monsoon followed by monsoon and post-monsoon seasons. For cycle I, pre-monsoon was dominant, and for cycle II, monsoon and post-monsoon were dominant. The high concentration of ion in non-monsoon season was attributed to anthropogenic impact and in the monsoon season to influx of run-off with influence of cyclic salts. In the Brahmaputra River, temporal variation of average anion concentration is in order: $HCO_3^- > SO_4^{2-} > Cl^- > H_4SiO_4 > NO_3^- > PO_4^{3-}$, and cation concentration is in the $Ca^{2+} > Mg^{2+} > Na^+ > K^+$ in all the seasons.
2. Analysis of variance (ANOVA) showed significant seasonal variations owing to contributions from weathering processes and differences in water discharges.
3. The water chemistry of Brahmaputra River is mainly controlled by rock weathering with minor contributions from atmospheric and anthropogenic sources. High average molar ratio of $(Ca^{2+} + Mg^{2+})/(Na^+ + K^+)$ and $(Na^+ + K^+)/Tz^+$ suggested contribution of ions through carbonate and silicate minerals.
4. The average precipitation-corrected molar ratio of (Ca^{2+}/Na^+), (HCO_3^-/Na^+) and (Mg^{2+}/Na^+) reflected influence of silicate and carbonate weathering.
5. Gibbs plot implied weathering as the major mechanism that controls the water chemistry of the Brahmaputra River. Ternary plot for cation and anion suggests dominance of carbonate and carbonate–evaporite–sulphide weathering
6. Factor analysis indicated that in pre-monsoon carbonate weathering and anthropogenic contamination are the governing processes which are replaced by silicate weathering in monsoon. Finally, in post-monsoon both carbonate and silicate weathering seem to be equally operative in the Brahmaputra River
7. Higher P_{CO_2} value than the atmospheric value indicates that disequilibrium exists in water bodies with the atmosphere which is due to the contribution of groundwater containing high CO_2 and the slow rate of its re-equilibrium.
8. Average silicate weathering rate (SWR) in the Brahmaputra River for cycle I was 6.50 tKm^{-2} $year^{-1}$ in pre-monsoon, 8.59 tKm^{-2} $year^{-1}$ in monsoon and 4.4 tKm^{-2} $year^{-1}$ in post-monsoon, and for cycle II, it is 5.29 tKm^{-2} $year^{-1}$ in pre-monsoon, 7.01 tKm^{-2} $year^{-1}$ in monsoon and 3.85 tKm^{-2} $year^{-1}$ in post-monsoon seasons. Average annual SWR was found to be high in monsoon season.
9. Average chemical weathering rate (CWR) in the Brahmaputra River was found to be 97.7 tKm^{-2} $year^{-1}$ in pre-monsoon, 66.4 tKm^{-2} $year^{-1}$ in monsoon and 56.3 tKm^{-2} $year^{-1}$ in post-monsoon for cycle I and 77.4 tKm^{-2} $year^{-1}$ in pre-monsoon, 55.0 tKm^{-2} $year^{-1}$ in monsoon and 48.5 tKm^{-2} $year^{-1}$ in post-monsoon for cycle II. Average CWR was found to be higher than previous finding. Rapid rock uplift and different physical erosion rate were responsible for high CWR in the Brahmaputra River
10. The average annual CO_2 consumption rate due to silicate weathering was found to be 0.52 ($\times 10^6$ mol Km^{-2} $year^{-1}$) and 0.49 ($\times 10^6$ mol Km^{-2} $year^{-1}$) for cycle I and cycle II, respectively. CO_2 consumption rate in the present study is significantly higher than the previous studies.

11. The average annual CO_2 consumption rate CO_2 consumption rate due to carbonate weathering of the Brahmaputra River was found to be 0.55 and 0.52 ($\times 10^6$ - mol Km^{-2} $year^{-1}$) for cycle I. Cycle II, respectively, shows increase value of (0.01×10^6 mol Km^{-2} $year^{-1}$). As compared with world's major rivers, the CO_2 consumption rate due to carbonate weathering of the Brahmaputra River was higher than that of the Ganga, Indus, Amazon, Huang He and lower than the Mekong River.
12. Estimation of chemical weathering rates of the Brahmaputra River indicated that carbonate weathering largely dominates the water chemistry of the river. High CO_2 consumption rate was associated with carbonate weathering

References

APHA (2005) Standard methods for the examination of water and waste water, 19th edn. American Public Health Association, Washington

Berner EK, Berner RA (1996) Global environment water, air, and geochemical cycles. Geochim Cosmochim Acta 1996(60):5157–5158

Berner RA, Lasaga AC, Garrels RM (1983) The carbonate–silicate geochemical cycle and its effect on atmospheric carbon dioxide over the past 100 million years. Am J Sci 284:641–683

Bu H, Tan X, Li S, Zhang Q (2010) Temporal and spatial variations of water quality in the Jinshui River of the South Qinling Mts, China. Ecotoxicol Environ Safety 73:907–913

Das A, Krishnaswami S, Sarin MM (2005) Chemical weathering in the Krishna Basin and Western Ghats of the Deccan Traps, India: rate of basalt weathering and their controls. Geochim Cosmochim Acta 66:3397–3416

Dessert C, Dupre B, Francoise LM, Schott J, Gaillardet J, Chakrapani GJ, Bajpai S (2001) Erosion of Deccan Traps determined by river geochemistry: impact on the global climate and the 87Sr/86Sr ratio of seawater. Earth Planet Sci Lett 188:459–474

Felipe-Sotelo M, Andrade JM, Carlosena A, Tauler R (2007) Temporal characterisation of river waters in urban and semi-urban areas using physico-chemical parameters and chemometric methods. Anal Chim Acta 583:128–137

Gaillardet J, Dupre B, Allegre CJ (1999) Global silicate weathering and CO_2 consumption rates deduced from the chemistry of large rivers. Chem Geol 159:3–30

Galy A, France-Lanord C (1999) Weathering processes in the Ganges Brahmaputra basin and the riverine alkalinity budget. Chem Geol 159:31–60

Gansser A (1964) Geology of the himalayas. Wiley Inter Science, London

Garrels RM, Mackenzie F (1971) Evolution of sedimentary rocks. Norton, New York

Gibbs RJ (1970) Mechanisms controlling world water chemistry. Science 4:170

Grasby SE, Hutcheon I (2000) Chemical dynamics and weathering rates of a carbonate basin Bow River, Southern Alberta. Appl Geochem 15:67–77

Gupta A (2008) Large rivers: geomorphology and management. Wiley, Hoboken

Horowitz AJ, Meybeck M, Idlafkih Z, Biger E (1999) Variations in trace element geochemistry in the Seine River Basin based on floodplain deposits and bed sediments. Hydrol Process 13:1329–1340

Hren MT, Chamberlain CP, Hilley GE, Blisniuk PM, Bookhagen B (2007) Major ion chemistry of the Yarlung Tsangpo-Brahmaputra River: chemical weathering, erosion and CO_2 consumption in the southern Tibetan plateau and eastern syntaxis of the Himalaya. Geochim Cosmochim Acta 71:2907.6–2935.6

Iler R (1979) The chemistry of silica: solubility, polymerization, colloid and surface properties and biochemistry. Wiley, New York

Jha PK, Tiwari J, Singh UK, Kumar M, Subramanian V (2009) Chemical weathering and associated CO_2 consumption in the Godavari river basin, India. Chem Geol 264:364–374

Jones JB et al (2003) Long-term decline in carbon dioxide super saturation in rivers across the contiguous United States. Geophys Res Lett 1:30

Krauskopf KB (1967) Introduction to Geochemistry. McGraw-Hill, New York

Krishnaswami S, Singh SK (2005) Chemical weathering in the river basins of the Himalaya, India. Curr Sci 89:841–849

Kumar M, Ramanathan AL, Keshari AK (2009a) Understanding the extent of interactions between groundwater and surface water through major ion chemistry and multivariate statistical techniques. Hydrol Process 23:297–310

Kumar M, Furumai H, Kurisu F, Kasuga I (2009b) Understanding the partitioning processes of mobile lead in soakaway sediments using sequential extraction and isotope analysis. Water Sci Technol 60(8):2085–2091

Li S, Lu XX, He M, Zhou Y, Bei R, Li L, Ziegler DA (2011) Major element chemistry in the upper Yangtze River: a case study of the Longchuanjiang River. Geomorphology 129:29–42

MacIntyre F (1970) Geochemical fractionation during mass transfer from sea to air by breaking bubbles. Tellus 22:451–462

Meybeck M (1983) Atmospheric inputs and river transport of dissolved substances, in symposium on dissolved loads of rivers. Int Ass Hydrol Sci Publ 141:119–173

Milliman JD, Meade RH (1983) World-wide delivery of river sediment to the oceans. J Geol 91:1–21

Millot R, Gaillardet J, Dupré B, Allégre CJ (2002) The global control of silicate weathering rates and the coupling with physical erosion: new insights from rivers of the Canadian Shield. Earth Planet Sci Lett 196:83–98

Rajasegar M (2003) Physico-chemical characteristics of the Vellar estuary in relation to shrimp farming. J Environ Biol 24:95–101

Raymo ME, Ruddiman WF, Froelich PN (1988) Influence of Late Cenozoic mountain building on ocean geochemical cycles. Geology 16:649–653

Roy S, Gaillerdet J, Allerge J (1999) Geochemistry of dissolved and suspended loads of the Seine river, France: anthropogenic impact, carbonate and silicate weathering. Geochim Cosmochim Acta 63:1277–1292

Sarin MM, Krishnaswami S, Dilli K, Somayajulu BLK, Moore WS (1989) Major ion chemistry of the Ganga-Brahmaputra River system: weathering processes and fluxes to the Bay of the Bengal. Geochim Cosmochim Acta 53:997–1009

Satsangi GS, Lakhani A, Khare P, Singh SP, Kumari KM, Srivastava SS (1998) Composition of rain water at a semiarid rural site in India. Atmos Environ 32:3783–3793

Sharma SK, Subramanian V (2008) Hydrochemistry of the Narmada and Tapti Rivers, India. Hydrol Process 22:3444–3455

Singh VP, Sharma N, Ojha CSP (2004) The Brahmaputra basin water Resource. Springer, Kluwer Academic Publishers, Berlin

Singh S, Sarin MM, France-Lanord C (2005) Chemical erosion in the eastern Himalaya: major ion composition of the Brahmaputra River and δ 13 C of dissolved inorganic carbon. Geochim Cosmochim Acta 69:3573–3588

Singh SK, Kumar A, France-Lanord C (2006) Sr and $^{87}Sr/^{86}Sr$ in waters and sediments of the Brahmaputra river system: Silicate weathering, CO_2 consumption and Sr flux. Chem Geol 234:308–320

Stallard RF, Edmond JM (1981) Geochemistry of the Amazon 1. Precipitation chemistry and the marine contribution to the dissolved load at the time of peak discharge. J Geophys Res 86:9844–9858

Subramanian V (2004) Water quality in south Asia. Asian J Water Environ Pollut 1:41–54

Subramanian V, Ittekkot V, Unger D, Madhavan N (2006) Silicate weathering in South Asian Tropical River Basins. The silicon cycle: human perturbations and impacts on aquatic systems. SCOPE series, 66. Island Press, Washington, D.C

Sun H, Han J, Li D, Zhang S, Lu XX (2010) Chemical weathering inferred from riverine water chemistry in the lower Xijiang basin, South China. Sci Total Environ 408:4749–4760

Thorne CR, Russell APG, Alam MK (1993) Planform pattern and channel evolution of the Brahmaputra River, Bangladesh. In: Best JL, Bristow CS (eds) Braided rivers. Geological Society, London, pp 257–276

Wadham JL, Hodson AJ, Tranter M, Dowdeswell JA (1998) The hydrochemistry of meltwater draining a polythermal-based, high Arctic glacier, south Svalbard. I: the ablation season. Hydrol Proc 12:1825–1849

Wu W, Xu S, Yang J, Yin H (2008) Silicate weathering and CO2 consumption deduced from seven Chinese rivers originating in the Qinghai-Tibet plateau. Chem Geol 249:307–320